



RESEARCH LETTER

10.1029/2022GL099577

Special Section:

Atmospheric Rivers: Intersection of Weather and Climate

Key Points:

- Antarctic-specific atmospheric river (AR) detection tools better capture continental interior footprint
- Modes of variability hold greater influence over West Antarctica than East Antarctica and are consistent across most AR detection tools
- Indian Ocean Dipole teleconnections in phase with El Niño Southern Oscillation produce a stronger AR precipitation response compared to other modes of natural variability

Supporting Information:

Supporting Information may be found in the online version of this article.

Correspondence to:

C. A. Shields,
shields@ucar.edu




Citation:

Shields, C. A., Wille, J. D., Marquardt Collow, A. B., MacLennan, M., & Gorodetskaya, I. V. (2022). Evaluating uncertainty and modes of variability for Antarctic atmospheric rivers. *Geophysical Research Letters*, 49, e2022GL099577. <https://doi.org/10.1029/2022GL099577>

Received 16 MAY 2022

Accepted 11 AUG 2022

Evaluating Uncertainty and Modes of Variability for Antarctic Atmospheric Rivers

Christine A. Shields¹ , Jonathan D. Wille² , Allison B. Marquardt Collow^{3,4}, Michelle MacLennan⁵ , and Irina V. Gorodetskaya⁶

¹Climate and Global Dynamics Laboratory, National Center for Atmospheric Research, Boulder, CO, USA, ²Institut des Géosciences de l'Environnement, CNRS/UGA/IRD/G-INP, Saint Martin d'Hères, France, ³University of Maryland Baltimore County, Baltimore, MD, USA, ⁴Global Modeling and Assimilation Office, NASA Goddard Space Flight Center, Greenbelt, MD, USA, ⁵Department of Atmospheric and Oceanic Science, University of Colorado Boulder, Boulder, CO, USA, ⁶Department of Physics, CESAM—Centre for Environmental and Marine Studies, University of Aveiro, Aveiro, Portugal

Abstract Antarctic atmospheric rivers (ARs) are driven by their synoptic environments and lead to profound and varying impacts along the coastlines and over the continent. The definition and detection of ARs over Antarctica accounts for large uncertainty in AR metrics, and consequently, impacts quantification. We find that Antarctic-specific detection tools consistently capture the AR footprint inland over ice sheets, whereas most global detection tools do not. Large-scale synoptic environments and associated ARs, however, are broadly consistent across detection tools. Using data from the Atmospheric River Tracking Method Intercomparison Project and global reanalyses, we quantify the uncertainty in Antarctic AR metrics and evaluate large-scale environments in the context of decadal and interannual modes of variability. The Antarctic western hemisphere has stronger connections to both decadal and interannual modes of variability compared to East Antarctica, and the Indian Ocean Dipole's influence on Antarctic ARs is stronger while in phase with El Niño Southern Oscillation.

Plain Language Summary Atmospheric rivers (ARs) are large-scale weather features that transport significant amounts of moisture and are akin to “rivers in the sky.” ARs traveling to Antarctica from the midlatitudes can bring enough moisture to produce extreme snowfall, or if accompanied by warm air, can result in melt events, both of which affect ice sheets across the continent. How we define ARs in gridded data sets significantly impact what we say about them. If a definition uses Antarctic-specific constraints, it does a better job at describing the actual spatial footprint for ARs impacting inland locales on the continent. The large-scale environments that produce ARs, and how these environments naturally vary, however, are generally consistent regardless of how we define ARs. ARs impacting the western hemisphere of Antarctica are more deeply connected to specific atmospheric patterns that repeatedly occur compared to weaker connections with East Antarctic ARs.

1. Introduction

Atmospheric rivers (ARs) are long, narrow synoptic-scale weather phenomena that serve as meridional transport vehicles important for large-scale and local hydrological climate across the globe. ARs transport both water and energy from lower to high latitudes and are often connected to extratropical cyclones where moisture laden bands of water vapor and clouds extend and travel across and along baroclinic zones (American Meteorological Society, 2017; Ralph et al., 2018). Although the bulk of the current literature describe ARs in midlatitude locations impacting western coasts of continents, such as western North America and western Europe, ARs are equally important in polar regions where the interaction of these moisture streams with land and sea ice, result in consequential precipitation events impacting the local cryosphere (Mattingly et al., 2018; Turner et al., 2019). Specific to Antarctica and depending on the thermal characteristics, ARs can produce significant snow accumulation over the ice sheet (Adusumilli et al., 2021; Gorodetskaya et al., 2014; Terpstra et al., 2021; Wille et al., 2021), or melt events with consequences for ice shelf stability (Clem et al., 2022; Turner et al., 2022; Wille et al., 2019, 2022). Generally, ARs reaching Antarctica are relatively rare occurrences (Wille et al., 2021), fully extending into the continent only a few times per year but clearly tied to favorable synoptic conditions, such as blocking events in the Southern Ocean that funnel ARs into the continent (Bozkurt et al., 2018; MacLennan & Lenaerts, 2021; Pohl et al., 2021; Terpstra et al., 2021; Wille et al., 2021). Despite their low frequency, they account for the largest

© 2022. The Authors.

This is an open access article under the terms of the [Creative Commons Attribution-NonCommercial-NoDerivs License](https://creativecommons.org/licenses/by-nc-nd/4.0/), which permits use and distribution in any medium, provided the original work is properly cited, the use is non-commercial and no modifications or adaptations are made.

percentage of total precipitation observed over Antarctica (Turner et al., 2019; Wille et al., 2021) and have important consequences for the continent's hydroclimate. ARs can also be tied to teleconnections and modes of natural variability (MOVs). AR occurrences for different regions around Antarctica have been attributed to various MOVs, such as the Southern Annular Mode (SAM) (Clem et al., 2016; Marshall & Thompson, 2016; Raphael et al., 2016; Wille et al., 2021), the Pacific South American Mode 2 (PSA2) (MacLennan et al., 2021; Marshall & Thompson, 2016), the Pacific Decadal Oscillation (PDO) (Fogt et al., 2019; Turner et al., 2019), the Indian Ocean Dipole and El Niño Southern Oscillation (IOD, ENSO) (Nuncio & Yuan, 2015). Parts of the cold temperature anomalies in West Antarctica can also be explained by the influence of the Indian Ocean Basin mode and Atlantic Zonal and Meridional Modes (Gutierrez et al., 2021; Lee & Jin, 2021; Li et al., 2015). In this study, we explicitly evaluate the relationship between these MOVs, ARs, and their associated precipitation and boundary layer temperature, to characterize the varied impacts across different regions and flavors of ARs. We do not evaluate surface impacts themselves, such as surface mass balance on glaciers, rather, we focus on understanding the large-scale variability that drives these impacts. Although we do not consider here an exhaustive list of MOVs of consequence for ARs, we limit this study to the decadal and interannual bimodal indices of variability introduced above. Additionally, because the very definition of an AR is often debated (i.e., is the feature simply a moisture transport alone, or rather, connected to an extratropical cyclone) (Gimeno et al., 2021; Ralph et al., 2018; Shields et al., 2019) we quantify the uncertainties in AR metrics such as occurrence and climatology, as well as MOV impact, to provide context for our results.

2. Data and Methods

2.1. Reanalysis Data Sets

We employ the Modern Era Retrospective Analysis for Research and Applications, v2 (MERRA-2) (Gelaro et al., 2017) and European Center for Medium-Range Weather Forecasts' Reanalysis Version 5 (ERA5) (Hersbach et al., 2020) global reanalyses. To represent large-scale synoptics and analyze modes of variability, we primarily use MERRA-2, which explicitly represents the energy and hydrologic budgets over ice sheets in Antarctica (Gelaro et al., 2017). An in-depth evaluation of the cryosphere in MERRA-2 is available in Section 9 of Bosilovich et al. (2015) and Gossart et al. (2019). Sea surface temperature and sea ice concentration in MERRA-2 are prescribed as indicated by Table 3 of Gelaro et al. (2017). At ~50 km resolution, MERRA-2 is sufficient to resolve weather features, such as atmospheric rivers, along with their associated precipitation, and is the baseline data set for the Atmospheric River Tracking Method Intercomparison Project (ARTMIP) (Rutz et al., 2019; Shields et al., 2018). ARTMIP provides a collection of AR “catalogs” from a variety of ARDTs (Atmospheric River Detection Tools) that detail gridded and timeslice information on where and when ARs exist. Using MERRA-2 across the same years as included in ARTMIP (1980–2016) allows us to consistently apply available ARTMIP ARDT catalogs to Antarctic AR uncertainty quantification. ERA5 data sets are also applied (1980–2020), where available, to further represent the spread in climatology metrics across both ARDT and reanalysis products and robustly quantify uncertainty by using as many catalogs as possible. Monthly MERRA-2 data are used to compute MOV indices (GMAO, 2015a; 2015b), daily data to compute precipitation (GMAO, 2015c), and 850 hPa temperature (GMAO, 2015d) for AR days, and 3-hourly data are used for AR identification (GMAO, 2015d). Only ARDTs with polar constraints (those that incorporate a lower threshold designed for polar latitudes, here referred to as P-ARTMIP) are used for MOV analysis to minimize errors by only including appropriately designed ARDTs.

2.2. Atmospheric River Detection

Identification and tracking of ARs require decisions dependent on the AR definition. Because this definition varies wildly from one project to another (Ralph et al., 2018; Rutz et al., 2019), metrics such as AR frequency and seasonality differ depending on choice of ARDT. ARTMIP has shown that uncertainty based on ARDT far outweighs uncertainty based on model (O'Brien et al., 2021) as well as reanalysis (Collow et al., 2022). Thus, uncertainty quantification is an important component to any analysis where AR detection is required. It is important to recognize that applying many different ARDTs for each science problem is not always practical for individual researchers, so a balance must be struck to address ARDT uncertainty, either by applying multiple ARDTs, such as this work and ARTMIP, or minimally, determining if the chosen ARDT is fit for purpose (Rutz et al., 2019). Traditional ARDTs designed for the midlatitudes typically apply moisture thresholds using the quantity called integrated vapor transport (IVT). However, for ARs making landfall and extending poleward onto the continent,

one option is to identify ARs by simply using the meridional component. Here, we apply Antarctic-specific ARDTs to diagnose the relationship between MOVs and ARs across Antarctica but include all methods with polar constraints to represent uncertainty spread. For climatology metrics, we include available global ARTMIP ARDTs to highlight the large differences in metrics. The Antarctic-specific algorithms, herein referred to as Wille_vIVT and Wille_IWV, focus on meridional geometry and filter for high (98% percentile) relative moisture flow into the continent to better capture ARs impacting polar latitudes, rather than zonally around the Southern Ocean. Details on Wille the ARDTs (Wille et al., 2019, 2021), ARTMIP ARDTs, and IVT/IWV calculations are in Supplemental.

2.3. Modes of Variability

We calculate both decadal and interannual modes of variability consistent with the Climate Variability and Diagnostic Package (CVDP) (Phillips et al., 2014). Modes were chosen based on the current literature with an already established or potential connection to AR impacts in and around Antarctica. Decadal modes are represented here by the SAM and the PDO, and for interannual modes, PSA2 and IOD, both in and out of phase with ENSO. All these indices have been found to influence both Antarctic precipitation and temperature (as summarized in Gutierrez et al. (2021), Table Atlas 1). Specific details on computation are found in Supplemental. One caveat to using the PDO is the relatively short time span of available data of ~four decades. Tropical Pacific decadal variability (TPDV) such as the PDO have timescales from 8 to 40 years (Power et al., 2021), making significance testing challenging. Because we are limited to the ARTMIP time period and thus only 37 years are used, PDO and AR correlations are shown for qualitative illustration, but significance inferences are limited and used with caution.

3. Climatological Characteristics and Uncertainty Due To ARDT

ARs impacting high latitude locales such as Antarctica do not necessarily follow midlatitude storm tracks. Rather, ARs often bend and flow around high-pressure blocks or follow baroclinic zones connected to low pressure regimes ultimately pushing moisture intrusions into the continent. ARs that make it onto the continent are dominated by the north-south meridional component of the wind (not shown). This can be demonstrated by computing heat maps of AR occurrence for each method and comparing the Antarctic-specific occurrences to traditional methods developed for midlatitudes. Figure 1a shows the spatial distribution differences between the mean Wille Antarctic-specific ARDTs and the ARTMIP mean. ARs that make landfall are generally rare (several per year, Wille et al., 2021), but even so, the Antarctic-specific ARDTs consistently detect ARs in the interior of the continent where most traditional ARDTs detect more in the Southern Ocean. Even global ARDTs that allow for polar thresholds (P-ARTMIP) (Figure 1b) ultimately do not capture ARs on the interior ice sheets, especially over East Antarctica. This is likely because the Antarctic-specific ARDTs applied here focus on the meridional component of the moisture transport that allows for AR detection deeper into the dry Antarctic interior.

From a continent-wide, climatological perspective (Figure 2), the Wille ARDTs detect ARs distributed throughout the year, with maximum occurrence in Austral fall and winter, consistent with instrumental observations and Regional Climate Model (RACMO2) that show high accumulation events with synoptic conditions for West Antarctica over Thwaites Glacier (~108.5°W) (Lenaerts et al., 2018; MacLennan et al., 2021) and East Antarctica over Dronning Maud Land (~20°W–45°E) (Gorodetskaya et al., 2013, 2014, 2020) (Antarctic geography in Figure S1 in Supporting Information S1). Distinctly different from Wille ARDTs, ARs detected from global and P-ARTMIP methods, peak in February and Austral Fall, and are likely due to the predominance of ARs impacting the Antarctic Peninsula, which in some cases, are the only location where ARs are identified (Figures S3 and S4 in Supporting Information S1). Because of the geographic position of the Peninsula in the Southern Ocean, the global ARDTs, designed for midlatitudes, capture more zonally oriented ARs. Specific regional climatologies (Antarctic Peninsula, Dronning Maud Land, and Princess Elizabeth/Queen Mary Lands, ~73°–100°E) are in Supplemental.

4. Relationship Between Antarctic ARs and MOVs

4.1. MOV Synoptics for AR Days

Around and across Antarctica, there are a variety of different climate regimes, but coastal climates depend on geometry and orientation of the coast relative to the zonal and meridional flow. However, for the purposes

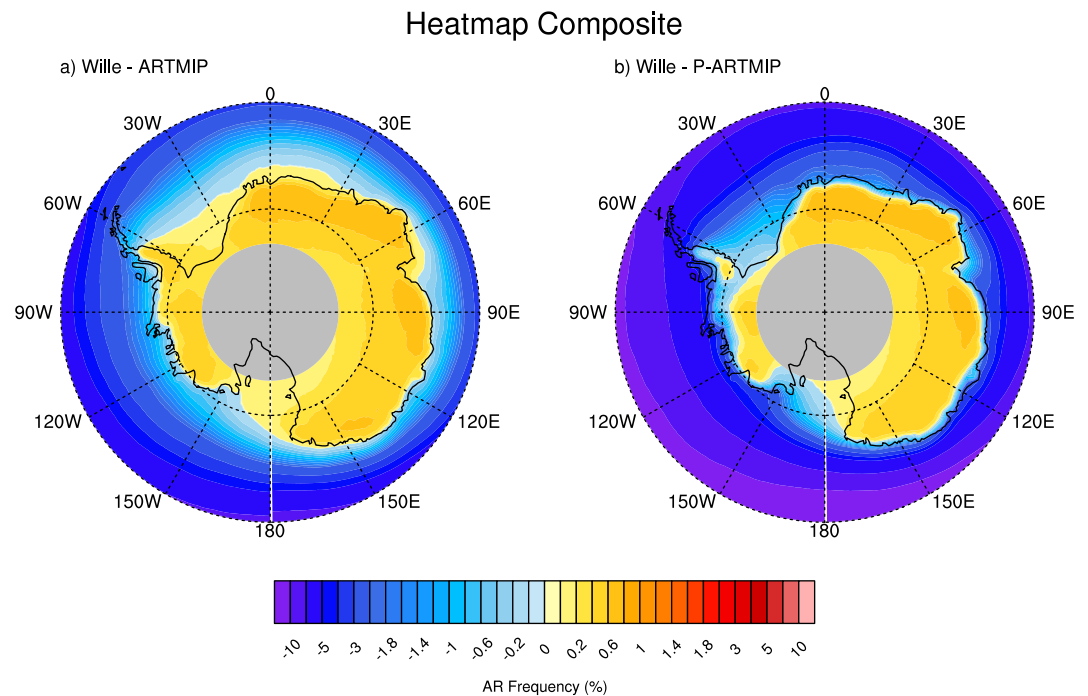


Figure 1. Composite difference heatmaps of atmospheric river (AR) frequency in % time (relative to full Atmospheric River Tracking Method Intercomparison Project Modern Era Retrospective Analysis for Research and Applications, v2 (ARTMIP MERRA-2) time span, 1980–2016). Wille Atmospheric River Detection Tools (ARDTs) versus applicable global ARDTs (a), Wille ARDTs versus P-ARTMIP (b).

of evaluating broad synoptic influences, we divide our study into West and East Antarctica. To isolate and amplify unique west and east hemispheric patterns, we apply the split hemisphere technique, commonly used for peak (seasonal) tropical cyclone track density analysis (Korty et al., 2012; Yan et al., 2016), except here, we composite synoptic conditions for landfalling ARs for respective hemisphere. That is, for days where

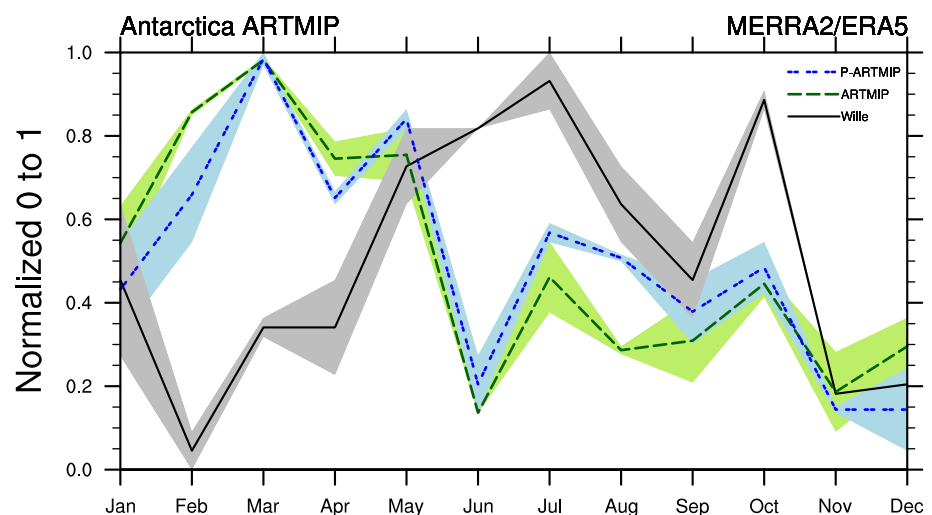


Figure 2. Antarctic seasonal cycle of Atmospheric rivers (ARs) for Atmospheric River Tracking Method Intercomparison Project (ARTMIP) mean (lines) and spread (shading) including applicable available Atmospheric River Detection Tools (ARDTs) (Table S1 and Figure S3 in Supporting Information S1) and both reanalysis data sets ARTMIP Tier 1 Modern Era Retrospective Analysis for Research and Applications, v2 (MERRA-2) and Tier two European Center for Medium-Range Weather Forecasts' Reanalysis Version 5 (ERA5). All global ARDTs (ARTMIP) versus ARTMIP with polar constraints (P-ARTMIP) versus Antarctic specific (Wille ARDTs).

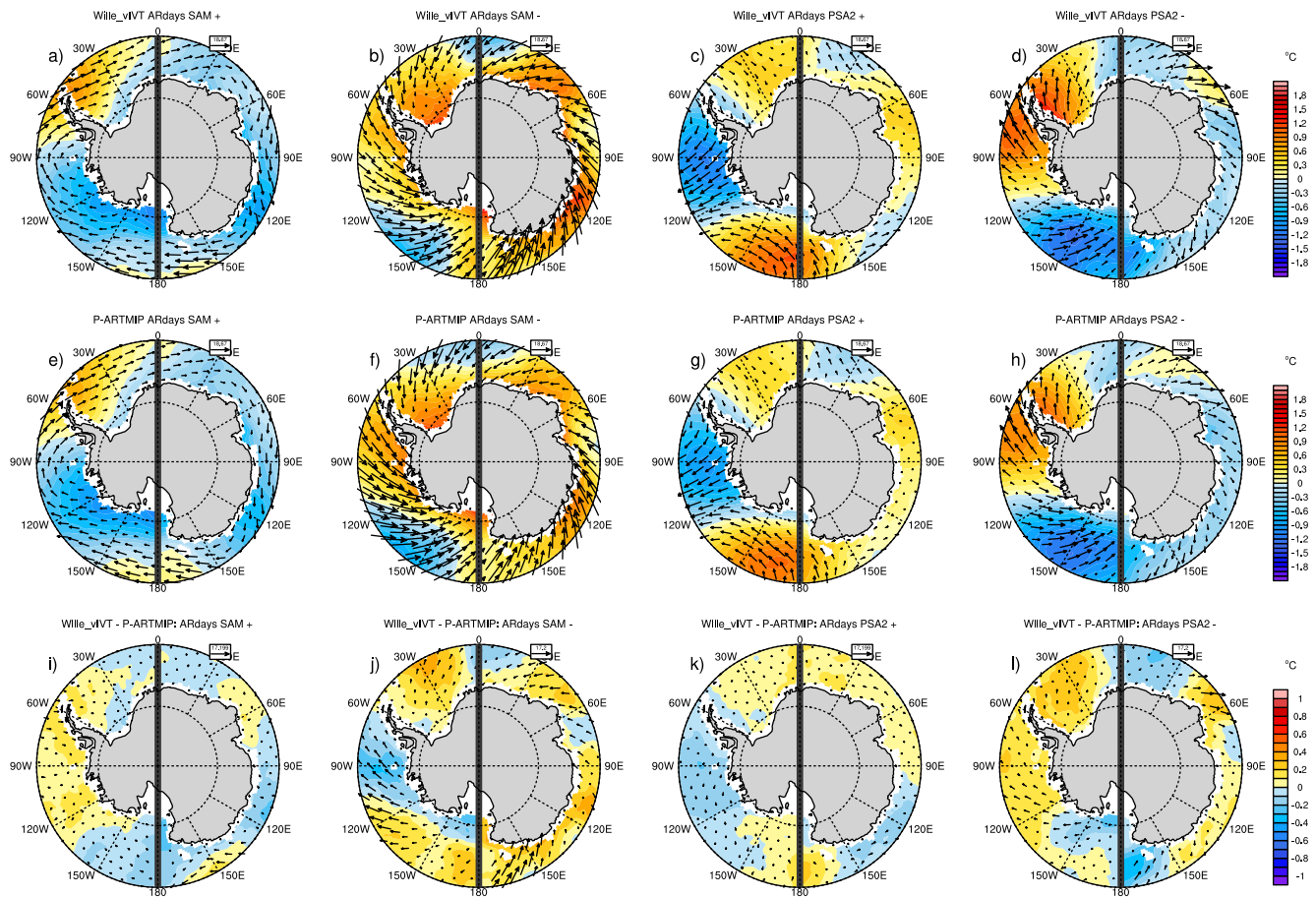


Figure 3. Anomalies of 850 hPa air temperature for atmospheric river (AR) day composites (color contours, °C) and 850 hPa moisture flux ($\text{kg m}^{-1} \text{s}^{-1}$) (arrows) during Southern Annular Mode (SAM) phases ((a, b), (e, f), and (i, j)), Pacific South American Mode 2 (PSA2) phases ((c, d), (g, h), and (k, l)) in split hemisphere format. West Antarctic ARs are composited separately from East Antarctic ARs to maintain unique hemispheric synoptic signatures, separated by thick gray line. Wille_vIVT (a–d), Atmospheric River Tracking Method Intercomparison Project (ARTMIP) mean for Atmospheric River Detection Tools (ARDTs) with polar constraints (P-ARTMIP) (e–h), differences (i–l). Reference vector is in the upper right box of each panel.

ARs impact West Antarctica, synoptic conditions are composited for the western hemisphere, and for days where ARs impact East Antarctica, synoptic conditions are composited for the eastern hemisphere. All spatial figures presented here contain a thick line as a reminder the hemispheres are treated separately but plotted together for illustration. We highlight the Wille_vIVT ARDT because this algorithm better represents AR dynamics (Wille et al., 2021). Figure 3 plots annual anomalies for 850 hPa moisture flux (vectors) and temperature (contours) for AR days occurring during the different phases of SAM and PSA, a decadal and interannual mode of variability, respectively, that represents variations in the dynamics. Across polar ARDTS (Figures 3e and 3h), fluxes in (SAM positive Antarctic Peninsula, PSA2 negative for the West Antarctic Ice Sheet, Amundsen and Ross Seas (Figure S1 in Supporting Information S1) and out of the continent for the western hemisphere, are consistent with Antarctic MOV patterns in Marshall and Thompson (2016) and Marshall et al. (2017). For East Antarctica, fluxes are varied but generally the opposite, with, for example, Dronning Maud Land showing fluxes into the continent during SAM negative. Overall PSA2 holds greater influence for the western hemisphere, and results are consistent across all global ARDTs, regardless of polar constraints or not (not shown). Across ARDTs for AR days, although there are variations in boundary layer temperature, moisture, and winds, synoptic conditions are robust across methods, unlike frequency metrics and seasonal climatology although some regional differences exist from Wille_vIVT (Figures 3i and 3l), our primary method. For example, SAM-, the Wille_vIVT ARDT detects more ARs with onshore flow ($\sim 180^\circ\text{--}150^\circ\text{E}$) to Terre Adelie Land ($\sim 140^\circ\text{E}$) (Figure 3j).

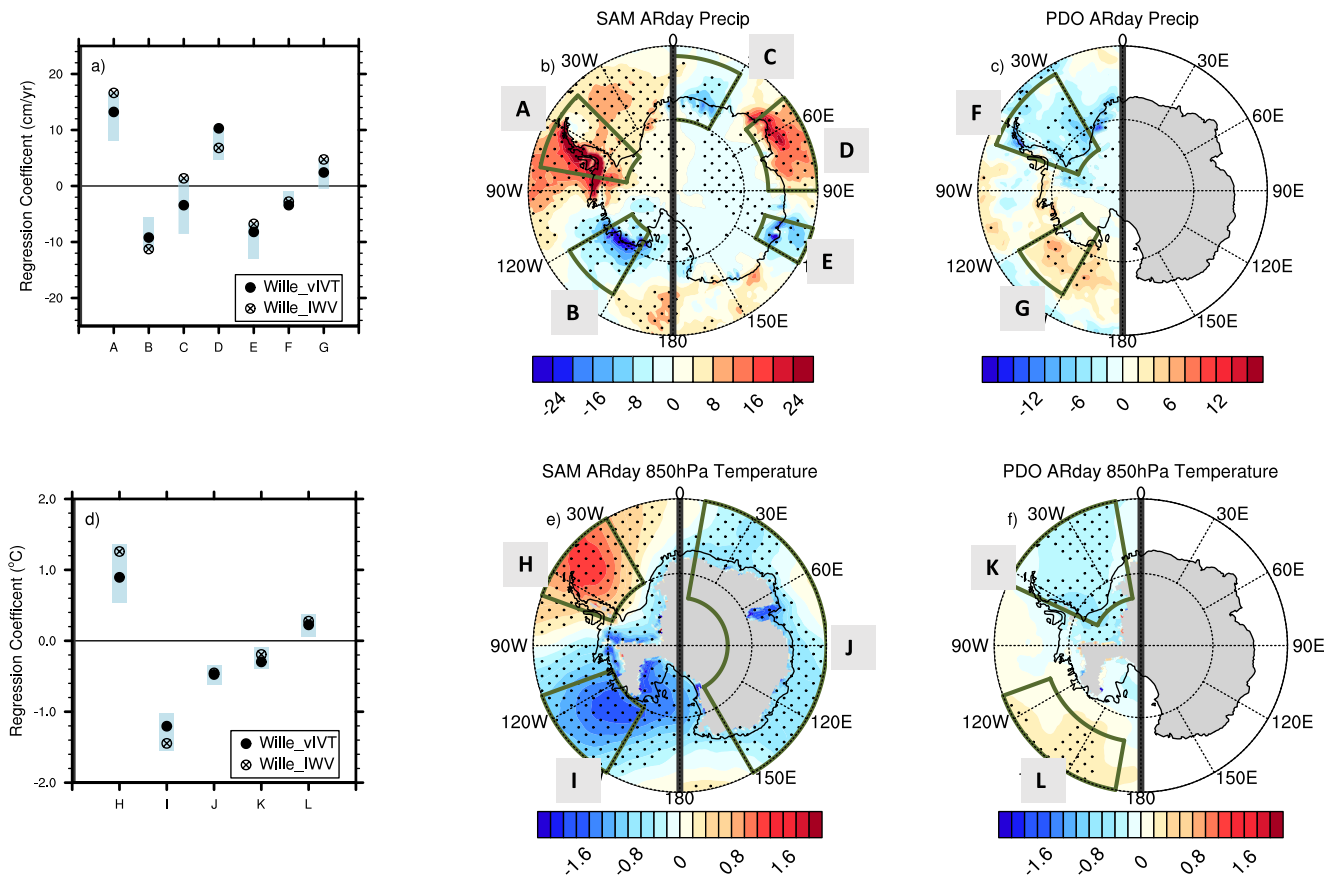


Figure 4. Regression patterns and spread for atmospheric river (AR) days and decadal modes of variability (Southern Annular Mode (SAM) and Pacific Decadal Oscillation (PDO)). Wille_vIVT precipitation (cm yr^{-1}) (b, c) and 850 hPa temperature ($^{\circ}\text{C}$) (e, f) patterns, split hemisphere format. Uncertainty is shown for area-averaged regression values across all P-ARTMIP ARDTs (blue shading, a, d). Dark green boxes indicate uncertainty area calculation and are labeled alphabetically. The PDO is shown for western hemisphere only. Significance was tested at 90% level, Student's t test. Where shown, 850 hPa temperatures are plotted for topographical regions under 850 hPa eliminating elevation errors on pressure surfaces.

4.2. Precipitation and Temperature Impacts

4.2.1. Decadal Modes of Variability: SAM and PDO

Decadal modes of variability, their relationship with AR precipitation and 850 hPa temperature, and ARTMIP uncertainty, are shown (Figure 4). We highlight the Wille_vIVT ARDT for spatial plots that regress PC time series for SAM (Figures 4b and 4e) and PDO (Figures 4c and 4f) onto precipitation and temperature anomalies for AR days. For the PDO, we show western hemisphere only due to the lack of any significance elsewhere. Precipitation and temperature follow the composite plots for AR days (Figure 3) in that where moisture fluxes flow into the continent, enhanced precipitation occurs, along with corresponding temperature anomalies. For example, SAM in the positive phase typically indicates a deeper Amundsen Sea Low (and vice versa), and generally less mass transport between Antarctica and the southern midlatitudes (Spensberger et al., 2020; Turner et al., 2013). Figure 4b shows the precipitation is positively and significantly correlated with SAM over Antarctic Peninsula (label A) and negatively correlated over the Amundsen sea region (label B), resulting from a deeper Amundsen Sea Low that brings cyclonic, clockwise flow into the Peninsula and out of the Amundsen sea region during SAM positive. SAM negative, oppositely correlated with precipitation between Amundsen and Ross Seas near Marie Byrd Land ($\sim 120^{\circ}\text{W}$), supports onshore flow during the negative phase. The eastern hemisphere shows less significance in precipitation although SAM's influence is hinted at in regions such as Dronning Maud Land, Kemp Land and the Amery Ice Shelf, and Wilkes Land (labels C, D, E, respectively; Figure S1 in Supporting Information S1 for Antarctic locations). The PDO shows a negative correlation with the Antarctic Peninsula in both temperature and precipitation (labels K, F), and a positive one between the Amundsen and Ross Seas (labels

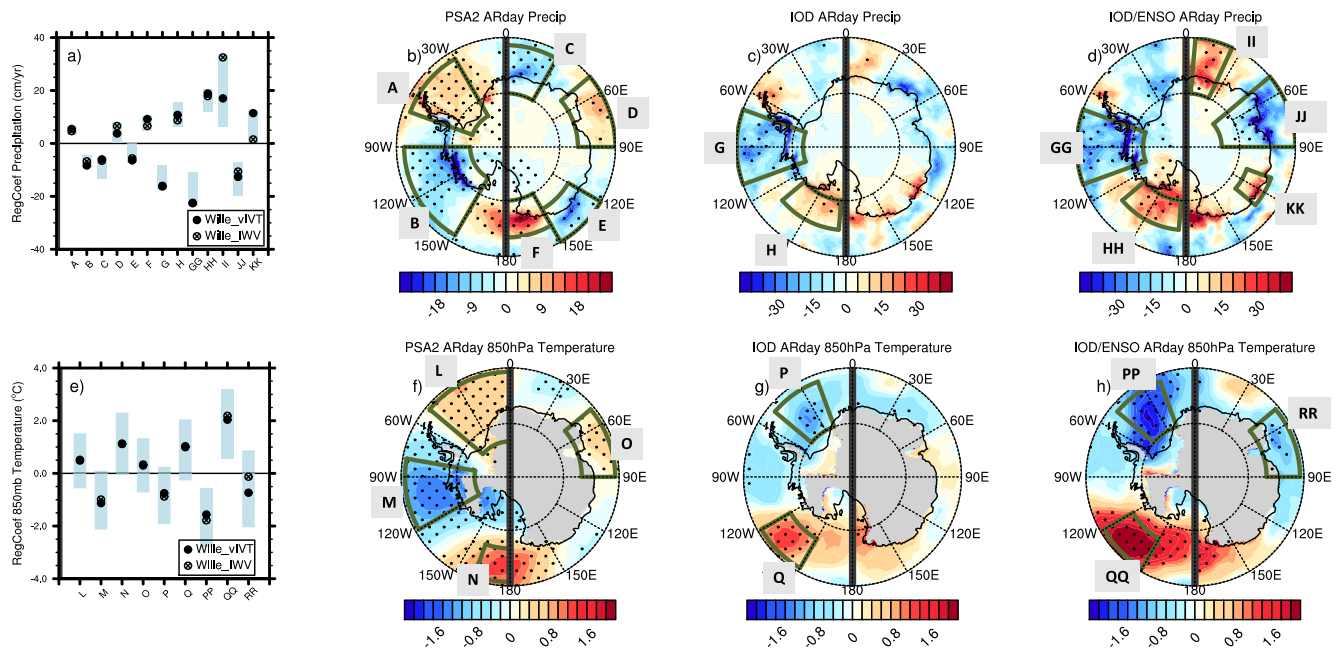


Figure 5. Same as Figure 4 except for interannual modes of variability Pacific South American Mode 2 (PSA2) (b, f), Indian Ocean Dipole (IOD) without (c, g) and IOD in phase with El Niño Southern Oscillation (ENSO) (d, h). Significance was tested at 90% level, Student's *t* test. Precipitation contour scales are different for PSA2 versus IOD.

L, G), although significance is weak and overall shows less influence than SAM. Each region that shows significance is tested across all P-ARTMIP algorithms (Figures 4a and 4d) to quantify uncertainty in these calculations. Across most regions and methods, the sign of the correlation is robust for both temperature and precipitation, except for Dronning Maud Land (DML) for precipitation (label C), where the strength of the correlation is generally tied to frequency climatology.

4.2.2. Interannual Modes of Variability: PSA2, IOD, and ENSO

Interannual modes of variability, their relationship with AR precipitation and 850 hPa temperature, and ARTMIP uncertainty, is shown in Figure 5. We evaluate PSA2 and IOD independently to illustrate their dominant, spatial impacts. However, it is important to note that no MOV, and especially interannual modes, operate in isolation. The PSA2 mode has been shown to excite sea surface temperature (SST) patterns tied to the evolution of ENSO (Lou et al., 2021), and the IOD is often paired with ENSO, in addition to decadal modes such as PDO. For simplicity, we evaluate the dynamical mode of PSA2 separately from modes defined by SST anomalies (IOD, ENSO). The PSA2 has already been shown to have significant implications for the Amundsen Sea Embayment and Thwaites Glacier (MacLennan & Lenaerts, 2021), and we confirm this with our regression analysis that shows negative correlation with PSA2 and precipitation in this area (label B), consistent with flux composites in Figure 3 and a potential amplification of wavenumber 3 (Cai et al., 1999). Temperature anomalies for AR days also align with regressions where poleward flow from midlatitudes brings warmth into the Ross Sea region and is positively correlated with PSA2 (label N) compared to equatorward flow, negative correlations, and colder temperature over Amundsen Sea (label M). The IOD (Figures 5c, 5d, and 5g, 5h) is more potent while in phase with ENSO with negative correlations over West Antarctic regions such as Ellsworth Land (labels GG, PP) and positive correlations with Eastern Dronning Maud Land (label II) and Ross Sea (labels HH, QQ). Temperature significance is stronger than precipitation significance, however, likely tied to the broad extratropical SST influences during these modes. Although significance with Wille_vIVT is strong for temperatures, the differences with Wille_IWV and the P-ARTMIP spread (Figures 5a and 5e) suggest this result is not necessarily robust across ARDTs, and potentially changes the sign of the correlation. Precipitation uncertainty is smaller, with most of the methods agreeing on correlation signs except for the IOD responses near Wilkes Land (label KK). Finally, the amplitude of IOD-ENSO response is much higher than any other MOV, interannual or decadal, suggesting that IOD in phase with ENSO produces more anomalous precipitation than any other mode studied here. Nuncio and

Yuan (2015) describe Antarctic sea ice correlations during IOD with ENSO in the Pacific sector and Ross Seas, and note the decrease in sea ice corresponding to warm meridional flow. Additionally, the wave train schematic in Nuncio and Yuan (2015) is consistent with our results that show for AR days, precipitation and warm low-level temperatures are positively correlated due to enhanced poleward flow at the Ross Sea and equatorward flow off the West Antarctic Ice Sheet.

5. Conclusions

Studying Antarctic atmospheric rivers combines a unique set of disciplines incorporating both atmospheric science and the cryosphere, but also cross-disciplinary interests such as feature detection. To understand this phenomenon, we must both define it and put it into context with current research. Antarctic AR detection tools are generally robust across the synoptic meteorology, however large uncertainties exist for AR frequency climatology metrics such as seasonal cycle and location of landfall. Antarctic-specific tools that rely on the meridional characteristics of ARs capture the continental interior footprint of ARs more consistently compared to global ARDTs designed for the midlatitudes. When evaluating ARs in the context of modes of natural variability (SAM, PSA2, PDO, IOD, and ENSO), this study finds the MOVs studied here influence West Antarctic ARs more than East Antarctica. Spread among ARDTs is generally smaller for decadal modes of variability compared to interannual modes. This is likely due to the shorter period for interannual modes and the opportunity for compounding MOV events. Additionally, the Indian Ocean Dipole teleconnections with ENSO produce a stronger AR response, mostly for West Antarctica and the Pacific sector, compared to other MOVs. Although we have chosen to diagnose MOVs that sample both decadal and interannual variability, it is not a complete list of potential influences on ARs onto the Antarctic glaciers and ice shelves. Future work includes understanding compound MOVs beyond IOD and ENSO. With our exploration of IOD and ENSO, compound MOVs clearly have the potential to amplify or suppress AR activity. Understanding the interplay between MOVs and ARs improves predictability and the ability to manage consequences as we move into a warmer climate. A future increase in MOVs that favor AR landfalls and warmer conditions will likely increase snowfall in the impacted area, but also risk increased surface melt and ice shelf destabilization.

Data Availability Statement

ARTMIP data are available from the Climate Data Gateway <https://doi.org/10.5065/D6R78D1M> and <http://doi.org/10.5065/D62R3QFS>. MERRA-2 is available from the Goddard Earth Sciences Data and Information Services Center (GES DISC) at <https://disc.gsfc.nasa.gov/>, DOI links <https://doi.org/10.5067/9SC1VNTWGWV3>, <https://doi.org/10.5067/Q5GVUVUIVGO7>. ERA5 data is available from the Copernicus Climate Change Service (C3S) Climate Data Store at <https://doi.org/10.24381/cds.adbb2d47>.

References

- Adusumilli, S., Fish, M. A., Fricker, H. A., & Medley, B. (2021). Atmospheric river precipitation contributed to rapid increases in surface height of the west Antarctic ice sheet in 2019. *Geophysical Research Letters*, *48*, e2020GL091076. <https://doi.org/10.1029/2020GL091076>
- American Meteorological Society. (2017). *Atmospheric river*. Glossary of Meteorology. Retrieved from http://glossary.ametsoc.org/wiki/Atmospheric_river
- Bosilovich, M. G., Akella, S., Coy, L., Cullather, R., Draper, C., Gelaro, R., et al. (2015). MERRA-2: Initial evaluation of the climate. *Technical Report Series on Global Modeling and Data Assimilation (NASA Tech. Rep. NASA/TM-2015-104606)*, (Vol. 43, p. 139). Greenbelt, MD: Goddard Space Flight Center. Retrieved from <https://gmao.gsfc.nasa.gov/pubs/docs/Bosilovich803.pdf>
- Bozkurt, D., Rondanelli, R., Marin, J. C., & Garreaud, R. (2018). Foehn event triggered by an atmospheric river underlies record-setting temperature along continental Antarctica. *Journal of Geophysical Research: Atmospheres*, *123*, 3871–3892. <https://doi.org/10.1002/2017JD027796>
- Cai, W., Baines, P. G., & Gordon, H. B. (1999). Southern mid-to high-latitude variability, a zonal wavenumber-3 pattern, and the Antarctic circumpolar wave in the CSIRO Coupled model. *Journal of Climate*, *12*(10), 3087–3104. [https://doi.org/10.1175/1520-0442\(1999\)012<3087:SMTHLV>2.0.CO;2](https://doi.org/10.1175/1520-0442(1999)012<3087:SMTHLV>2.0.CO;2)
- Clem, K. R., Bozkurt, D., Kennett, D., King, J. C., & Turner, J. (2022). Central tropical Pacific convection drives extreme high temperatures and surface melt on the Larsen C Ice Shelf, Antarctic Peninsula. *Nature Communications*, *13*, 3906. <https://doi.org/10.1038/s41467-022-31119-4>
- Clem, K. R., Renwick, J. A., McGregor, J., & Fogt, R. L. (2016). The relative influence of ENSO and SAM on Antarctic Peninsula climate. *Journal of Geophysical Research: Atmospheres*, *121*, 9324–9341. <https://doi.org/10.1002/2016JD025305>
- Collow, A. B. M., Shields, C. A., Guan, B., Kim, S., Lora, J. M., McClenny, E. E., et al. (2022). An overview of ARTMIP's Tier 2 Reanalysis Intercomparison: Uncertainty in the detection of atmospheric rivers and their associated precipitation. *Journal of Geophysical Research: Atmospheres*, *127*, e2021JD036155. <https://doi.org/10.1029/2021JD036155>
- Fogt, R. L., Schneider, D. P., & Goergens, C. A. (2019). Seasonal Antarctic pressure variability during the twentieth century from spatially complete reconstructions and CAM5 simulations. *Climate Dynamics*, *53*, 1435–1452. <https://doi.org/10.1007/s00382-019-04674-8>

Acknowledgments

This work is supported by the U.S. Department of Energy, Office of Science, Office of Biological & Environmental Research (BER), Regional and Global Model Analysis (RGMA) component of the Earth and Environmental System Modeling Program under Award Number DE-SC0022070 and National Science Foundation (NSF) IA 1947282 and by the National Center for Atmospheric Research (NCAR), sponsored by the NSF Cooperative Agreement No. 1852977. ARTMIP is a grass-roots community effort. Details on ARDTs can be found on the ARTMIP website, <https://www.cgd.ucar.edu/projects/artmip/algorithms.html>, but we specifically thank B. Guan, J. Lora, M. Krinsky, K. Kashinath, E. McClenny, K. Nardi, M. Pan, K. Reid, J. Rutz, T. O'Brien, E. Shearer, P. Ullrich, G. Xu) for their catalogs. ARTMIP DOE (BER) RGMA and the Center for Western Weather and Water Extremes (CW3E) at Scripps Institute for Oceanography at the University of California, San Diego. J. D. W. acknowledges support from the Agence Nationale de la Recherche project, ANR-20-CE01-0013 (ARCA). M. L. MacLennan acknowledges support from NASA FINESST Grant 80NSSC21K1610.

- Gelaro, R., McCarty, W., Suárez, M. J., Todling, R., Molod, A., Takacs, L., et al. (2017). The modern-Era retrospective analysis for research and applications, version 2 (MERRA-2). *Journal of Climate*, 30(14), 5419–5454. <https://doi.org/10.1175/JCLI-D-16-0758.1>
- Gimeno, L., Algarra, I., Eiras-Barca, J., Ramos, A. M., & Nieto, R. (2021). Atmospheric river, a term encompassing different meteorological patterns. *Wiley Interdisciplinary Reviews: Water*, 8(6), e1558. <https://doi.org/10.1002/wat2.1558>
- Global Modeling, & Assimilation Office (GMAO) (2015b). *MERRA-2 tavgM_2d_ocn_Nx: 2d, monthly mean, time-averaged, single-level, assimilation, ocean surface diagnostics V5.12.4*. Goddard Earth Sciences Data and Information Services Center (GES DISC). <https://doi.org/10.5067/4IASLIDL8EEC>
- Global Modeling, & Assimilation Office (GMAO) (2015c). *MERRA-2 tavg1_2d_flux_Nx: 2d, 1-hourly, time-averaged, single-level, assimilation, surface flux diagnostics V5.12.4*. Goddard Earth Sciences Data and Information Services Center (GES DISC). <https://doi.org/10.5067/7MCPBJ41Y0K6>
- Global Modeling, & Assimilation Office (GMAO) (2015d). *MERRA-2 inst3_3d_asm_Np: 3d, 3-hourly, instantaneous, pressure-level, assimilation, assimilated meteorological fields V5.12.4*. Goddard Earth Sciences Data and Information Services Center (GES DISC). <https://doi.org/10.5067/QBZ6MG944HW0>
- Global Modeling, & Assimilation Office (GMAO). (2015a). *MERRA-2 tavgM_2d_slv_Nx: 2d, monthly mean, time-averaged, single-level, assimilation, single-level diagnostics V5.12.4*. Goddard Earth Sciences Data and Information Services Center (GES DISC). <https://doi.org/10.5067/APIB0BA5PD2K>
- Gorodetskaya, I. V., Silva, T., Schmithüsen, H., & Hirasawa, N. (2020). Atmospheric river signatures in radiosonde profiles and reanalyses at the Dronning Maud land coast, east Antarctica. *Advances in Atmospheric Sciences*, 37(5), 455–476. <https://doi.org/10.1007/s00376-020-9221-8>
- Gorodetskaya, I. V., Tsukernik, M., Claes, K., Ralph, M. F., Neff, W. D., & VanLipzig, N. P. M. (2014). The role of atmospheric rivers in anomalous snow accumulation in East Antarctica. *Geophysical Research Letters*, 41, 6199–6206. <https://doi.org/10.1002/2014GL060881>
- Gorodetskaya, I. V., Van Lipzig, N. P. M., Vanden Broeke, M. R., Mangold, A., Boot, W., & Reijmer, C. H. (2013). Meteorological regimes and accumulation patterns at Utsteinen, Dronning Maud land, east Antarctica: Analysis of two contrasting years. *Journal of Geophysical Research: Atmospheres*, 118, 1700–1715. <https://doi.org/10.1002/jgrd.50177>
- Gossart, A., Helsen, S., Lenaerts, J. T. M., Broucke, S. V., van Lipzig, N. P. M., & Souverijns, N. (2019). An evaluation of surface climatology in State-of-the-art reanalyses over the Antarctic ice sheet. *Journal of Climate*, 32(20), 6899–6915. <https://doi.org/10.1175/JCLI-D-19-0030.1>
- Gutiérrez, J. M., Jones, R. G., Narisma, G. T., Alves, L. M., Amjad, M., Gorodetskaya, I. V., et al. (2021). Atlas. In V. Masson-Delmotte, P. Zhai, A. Pirani, S. L. Connors, C. Péan, S. Berger, et al. (Eds.), *Climate change 2021: The physical science basis. Contribution of working group I to the sixth assessment report of the intergovernmental panel on climate change* (pp. 1927–2058). Cambridge University Press. <https://doi.org/10.1017/9781009157896.021>
- Hersbach, H., Bell, B., Berrisford, P., Hirahara, S., Horányi, A., Muñoz-Sabater, J. (2020). The ERA5 global reanalysis. *Quarterly Journal of the Royal Meteorological Society*, 146, 1999–2049. <https://doi.org/10.1002/qj.3803>
- Korty, R. L., Camargo, S. J., & Galewsky, J. (2012). Variations in tropical cyclone Genesis Factors in simulations of the Holocene Epoch. *Journal of Climate*, 25(23), 8196–8211. <https://doi.org/10.1175/JCLI-D-12-00033.1>
- Lee, H.-J., & Jin, E.-K. (2021). Seasonality and dynamics of atmospheric teleconnection from the tropical Indian ocean and the Western Pacific to West Antarctica. *Atmosphere*, 12, 849. <https://doi.org/10.3390/atmos12070849>
- Lenaerts, J. T. M., Ligtenberg, S. R., Medley, B., Van De Berg, W. J., Konrad, H., & Nicolas, J. P. (2018). Climate and surface mass balance of coastal West Antarctica resolved by regional climate modelling. *Annals of Glaciology*, 59(76 pt 1), 29–41. <https://doi.org/10.1017/aog.2017.42>
- Li, X., Gerber, E. P., Holland, D. M., & Yoo, C. (2015). A Rossby wave bridge from the tropical Atlantic to West Antarctica. *Journal of Climate*, 28(6), 2256–2273. <https://doi.org/10.1175/JCLI-D-14-00450.1>
- Lou, J., O’Kane, T. J., & Holbrook, N. J. (2021). Linking the atmospheric Pacific-South American mode with oceanic variability and predictability. *Communications Earth & Environment*, 2, 223. <https://doi.org/10.1038/s43247-021-00295-4>
- MacIennan, M. L., & Lenaerts, J. T. (2021). Large-scale atmospheric drivers of snowfall over Thwaites Glacier, Antarctica. *Geophysical Research Letters*, 48, e2021GL093644. <https://doi.org/10.1029/2021GL093644>
- Marshall, G. J., Thompson, D. W., & van den Broeke, M. R. (2017). The signature of Southern Hemisphere atmospheric circulation patterns in Antarctic precipitation. *Geophysical Research Letters*, 44, 11–580. <https://doi.org/10.1002/2017GL075998>
- Marshall, G. J., & Thompson, D. W. J. (2016). The signatures of large-scale patterns of atmospheric variability in Antarctic surface temperatures. *Journal of Geophysical Research: Atmospheres*, 121, 3276–3289. <https://doi.org/10.1002/2015JD024665>
- Mattingly, K. S., Mote, T. L., & Fettweis, X. (2018). Atmospheric river impacts on Greenland Ice Sheet surface mass balance. *Journal of Geophysical Research: Atmospheres*, 123(16), 8538–8560. <https://doi.org/10.1029/2018JD028714>
- Nuncio, M., & Yuan, X. (2015). The influence of the Indian ocean dipole on Antarctic sea ice. *Journal of Climate*, 28(7), 2682–2690. <https://doi.org/10.1175/JCLI-D-14-00390.1>
- O’Brien, T. A., Wehner, M. F., Payne, A. E., Shields, C. A., Rutz, J. J., Leung, L. R., et al. (2021). Increases in future AR Count and size: Overview of the ARTMIP tier 2 CMIP5/6 Experiment. *Journal of Geophysical Research: Atmospheres*, 127, e2021JD036013. <https://doi.org/10.1029/2021JD036013>
- Phillips, A. S., Deser, C., & Fasullo, J. (2014). A new tool for evaluating modes of variability in climate models. *EOS*, 95, 453–455. <https://doi.org/10.1002/2014EO490002>
- Pohl, B., Favier, V., Wille, J., Udy, D. G., Vance, T. R., Pergaud, J., et al. (2021). Relationship between weather regimes and atmospheric rivers in East Antarctica. *Journal of Geophysical Research: Atmospheres*, 126, e2021JD035294. <https://doi.org/10.1029/2021JD035294>
- Power, S., Lengaigne, M., Capotondi, A., Khodri, M., Vialard, J., Jebri, B., et al. (2021). Decadal climate variability in the tropical Pacific: Characteristics, causes, predictability, and prospects. *Science*, 374(6563), eaay9165. <https://doi.org/10.1126/science.aay9165>
- Ralph, F. M., Dettinger, M. D., Cairns, M. M., Galarneau, T. J., & Eylander, J. (2018). Defining “atmospheric river”: How the glossary of meteorology helped resolve a debate. *Bulletin of the American Meteorological Society*, 99(4), 837–839. <https://doi.org/10.1175/BAMS-D-17-0157.1>
- Raphael, M. N., Marshall, G. J., Turner, J., Fogt, R. L., Schneider, D., Dixon, D. A., et al. (2016). The Amundsen Sea low: Variability, change, and impact on Antarctic climate. *Bulletin of the American Meteorological Society*, 97(1), 111–121. <https://doi.org/10.1175/BAMS-D-14-00018.1>
- Rutz, J. J., Shields, C. A., Lora, J. M., Payne, A. E., Guan, B., Ullrich, P., et al. (2019). The Atmospheric River Tracking Method Intercomparison Project (ARTMIP): Quantifying uncertainties in atmospheric river climatology. *Journal of Geophysical Research: Atmospheres*, 124, 13777–13802. <https://doi.org/10.1029/2019JD030936>
- Shields, C. A., Rutz, J. J., Leung, L. R., Ralph, F. M., Wehner, M., O’Brien, T., & Pierce, R. (2019). Defining uncertainties through comparison of atmospheric river tracking methods. *The Bulletin of the American Meteorological Society*, 100(2), ES93–ES96. <https://doi.org/10.1175/BAMS-D-18-0200.1>

- Shields, C. A., Rutz, J. J., Leung, L.-Y., Ralph, F. M., Wehner, M., Kawzenuk, B., et al. (2018). Atmospheric river tracking method Intercomparison project (ARTMIP): Project goals and experimental design. *Geoscientific Model Development*, *11*, 2455–2474. <https://doi.org/10.5194/gmd-11-2455-2018>
- Spensberger, C., Reeder, M. J., Spengler, T., & Patterson, M. (2020). The connection between the southern Annular mode and a feature-based perspective on southern hemisphere midlatitude winter variability. *Journal of Climate*, *33*(1), 115–129. <https://doi.org/10.1175/JCLI-D-19-0224.1>
- Terpstra, A., Gorodetskaya, I. V., & Sodemann, H. (2021). Linking sub-tropical evaporation and extreme precipitation over East Antarctica: An atmospheric river case study. *Journal of Geophysical Research: Atmospheres*, *126*, e2020JD033617. <https://doi.org/10.1029/2020JD033617>
- Turner, J., Lu, H., King, J. C., Carpentier, S., Lazzara, M., Phillips, T., & Wille, J. (2022). An extreme high temperature event in coastal East Antarctica associated with an atmospheric river and record summer downslope winds. *Geophysical Research Letters*, *49*, e2021GL097108. <https://doi.org/10.1029/2021GL097108>
- Turner, J., Marshall, G. J., Clem, K., Colwell, S., Phillips, T., & Lu, H. (2019). Antarctic temperature variability and change from station data. *International Journal of Climatology*, *40*, 2986–3007. <https://doi.org/10.1002/joc.6378>
- Turner, J., Phillips, T., Hosking, J. S., Marshall, G. J., & Orr, A. (2013). The Amundsen sea low. *International Journal of Climatology*, *33*(7), 1818–1829. <https://doi.org/10.1002/joc.3558>
- Wille, J. D., Favier, V., Dufour, A., Gorodetskaya, I. V., Turner, J., Agosta, C., & Codron, F. (2019). West Antarctic surface melt triggered by atmospheric rivers. *Nature Geoscience*, *12*, 911–916. <https://doi.org/10.1038/s41561-019-0460-1>
- Wille, J. D., Favier, V., Gorodetskaya, I. V., Agosta, C., Kittel, C., Beeman, J. C., et al. (2021). Antarctic atmospheric river climatology and precipitation impacts. *Journal of Geophysical Research: Atmospheres*, *126*, e2020JD033788. <https://doi.org/10.1029/2020JD033788>
- Wille, J. D., Favier, V., Jourdain, N. C., Kittel, C., Turton, J. V., Agosta, C. et al. (2022). Intense atmospheric rivers can weaken ice shelf stability at the Antarctic Peninsula. *Communications Earth & Environment*, *3*, 90. <https://doi.org/10.1038/s43247-022-00422-9>
- Yan, Q., Wei, T., Korty, R. L., Kossin, J. P., Zhang, Z., & Wang, H. (2016). Enhanced intensity of global tropical cyclones during the mid-Pliocene warm period. *Proceedings of the National Academy of Sciences of the United States of America*, *113*(46), 12963–12967. <https://doi.org/10.1073/pnas.1608950113>

References From the Supporting Information

- Guan, B., & Waliser, D. E. (2015). Detection of atmospheric rivers: Evaluation and application of an algorithm for global studies. *Journal of Geophysical Research: Atmospheres*, *120*, 514–535. <https://doi.org/10.1002/2015JD024257>
- Kashinath, K., Mudigonda, M., Kim, S., Kapp-Schwoerer, L., Graubner, A., Karaismailoglu, E., et al. (2021). ClimateNet: An expert-labeled open dataset and deep learning architecture for enabling high-precision analyses of extreme weather. *Geoscientific Model Development*, *14*(1), 107–124.
- Mundhenk, B. D., Barnes, E. A., & Maloney, E. D. (2016). All-season climatology and variability of atmospheric river frequencies over the North Pacific. *Journal of Climate*, *29*, 4885–4903. <https://doi.org/10.1175/JCLI-D-15-0655.1>
- O'Brien, T. A., Risser, M. D., Loring, B., Elbashaandy, A. A., Krishnan, H., Johnson, J., et al. (2020). Detection of atmospheric rivers with inline uncertainty quantification: TECA-BARD v1.0.1. *Geoscientific Model Development*, *13*(12), 6131–6148.
- Pan, M., & Lu, M. (2019). A novel atmospheric river identification algorithm. *Water Resources Research*, *55*, 6069–6087. <https://doi.org/10.1029/2018WR024407>
- Reid, K. J., King, A. D., Lane, T. P., & Short, E. (2020). The sensitivity of atmospheric river identification to integrated water vapor transport threshold, resolution, and regridding method. *Journal of Geophysical Research: Atmospheres*, *125*, e2020JD032897. <https://doi.org/10.1029/2020JD032897>
- Rutz, J. J., Steenburgh, W. J., & Ralph, F. M. (2014). Climatological characteristics of atmospheric rivers and their inland penetration over the Western United States. *Mon. Wea. Rev.*, *142*, 905–921. <https://doi.org/10.1175/mwr-d-13-00168.1>
- Shearer, E. J., Nguyen, P., Sellars, S. L., Analui, B., Kawzenuk, B., Hsu, K., et al. (2020). Examination of global midlatitude atmospheric river lifecycles using an object-oriented methodology. In *Journal of Geophysical Research: Atmospheres* (Vol. 125). <https://doi.org/10.1029/2020jd033425e2020JD033425>
- Skinner, C. B., Lora, J. M., Payne, A. E., & Pouslen, C. J. (2020). Atmospheric river changes shaped mid-latitude hydroclimate since the mid-holocene. *Earth and Planetary Science Letters*, *541*, 116293. <https://doi.org/10.1016/j.epsl.2020.116293>
- Ullrich, P. A., & Zarzycki, C. M. (2017). TempestExtremes: A framework for scale-insensitive pointwise feature tracking on unstructured grids. *Geoscientific Model Development*, *10*(3), 1069–1090. <https://doi.org/10.5194/gmd-10-1069-2017>